Journal of Magnetic Resonance 279 (2017) 29–38

Contents lists available at ScienceDirect

Journal of Magnetic Resonance

journal homepage: www.elsevier.com/locate/jmr

Parameterization of NMR relaxation curves in terms of logarithmic moments of the relaxation time distribution

Oleg V. Petrov *, Siegfried Stapf

Ilmenau University of Technology, 98693 Ilmenau, Germany

ARTICLE INFO

Article history:
Received 22 March 2017
Accepted 11 April 2017
Available online 13 April 2017

Keywords:
T_1 relaxometry
Field-cycling relaxometry
Non-exponential relaxation
Logarithmic moments
Laplace inversion
Stretched exponential fit

ABSTRACT

This work addresses the problem of a compact and easily comparable representation of multi-exponential relaxation data. It is often convenient to describe such data in a few parameters, all being of physical significance and easy to interpret, and in such a way that enables a model-free comparison between different groups of samples. Logarithmic moments (LMs) of the relaxation time constitute a set of parameters which are related to the characteristic relaxation time on the log-scale, the width and the asymmetry of an underlying distribution of exponentials. On the other hand, the calculation of LMs does not require knowing the actual distribution function and is reduced to a numerical integration of original data. The performance of this method has been tested on both synthetic and experimental NMR relaxation data which differ in a signal-to-noise ratio, the sampling range and the sampling rate. The calculation of two lower-order LMs, the log-mean time and the log-variance, has proved robust against deficiencies of the experiment such as scattered data point and incomplete sampling. One may consider using them as such to monitor formation of a heterogeneous structure, *e.g.*, in phase separation, vitrification, polymerization, hydration, aging, contrast agent propagation processes. It may also assist in interpreting frequency and temperature dependences of relaxation, revealing a crossover from slow to fast exchange between populations. The third LM was found to be a less reliable quantity due to its susceptibility to the noise and must be used with caution.

1. Introduction

A non-exponential NMR relaxation behavior is often attributed to dynamically heterogeneous systems with distinguishable populations characterized by individual relaxation times, τ_i's. Mathematically, it is expressed in terms of relaxation time distribution, $g(\tau)$, or relaxation spectrum. The concept of the relaxation time distribution has been employed since the early 1990, mostly in connection with pore size distribution in rocks [1,2]. More recently, it has been studied with regard to its correlation with a chain length distribution in crude oils [3]. A quasi-continuous $g(\tau)$ is obtained through the Inverse Laplace Transform (ILT) of a relaxation function $\varphi(t)$ representing either decaying or recovering magnetization curves. While often criticized for non-unique solution and an inherent broadening of the resultant $g(\tau)$, ILT becomes a standard practice for multi-exponential relaxation data presentation, all the more so as reliable ILT algorithms reach the NMR community [4,5].

For intrinsically non-exponential relaxation in a homogeneous medium, one has to use another approach and fit to data a function, either empirical or derived within an appropriate dynamics model, the parameters of which are related to a characteristic time of relaxation and its deviation from an exponential. Kohlrausch and log-normal fit functions are but two of the examples. It has been shown, however, that a monotone non-exponential $\varphi(t)$ can be always approximated arbitrarily closely by a sum of exponentials with an appropriate $g(\tau)$ [6]. This makes the description of relaxation in terms of $g(\tau)$ a general concept on the understanding that it underlies a non-exponential $\varphi(t)$ of a particular kind.

ILT provides an ultimate description of multi-exponential data in the sense that $g(\tau)$ uniquely determines $\varphi(t)$. It is often the case, however, that one utilizes thus-obtained $g(\tau)$ only to measure a certain numerical quantity, in order to relate it to another sample's property, or to monitor the change of relaxation upon varying experimental conditions and to assess a trend in the relaxation behavior, or merely to catalog a sample according to this quantity. What is often considered in such a case are the average relaxation time, the width of $g(\tau)$, and the skewness of $g(\tau)$. Zorn [7] has advocated the presentation of these properties of $g(\tau)$ through lower-order moments of the relaxation time. He has shown, on

* Corresponding author.
E-mail address: oleg.petrov@tu-ilmenau.de (O.V. Petrov).

http://dx.doi.org/10.1016/j.jmr.2017.04.009
1090-7807/

the example of dielectric relaxation, that the moments can be evaluated directly from the relaxation function, that is, without knowing $g(\tau)$ from data inversion, when the function is sampled in logarithmically equispaced steps.

The demand for skipping data inversion in numerical relaxation analysis, thus avoiding ambiguities that may accompany such inversion, was met earlier in [8] in the context of computations of different average NMR relaxation times.

Ref. [7] provides necessary basis for calculating the moments on the log-scale (hereafter called logarithmic moments) and gives analytical expressions for a number of empirical fit functions used in dielectric relaxometry (both in time and frequency domain). Here we adapt this approach for the analysis of experimental relaxation functions in time-domain NMR. Among the chief challenges of applying this approach to experimental data is a proper normalization of $\varphi(t)$, which relies on both the signal-to-noise ratio (SNR) and sampling completeness. Hence we validate this approach by testing its performance on relaxation functions (both synthetic and experimental) of various SNRs and numbers of sampling points acquired over different time intervals. To be concrete, we hereafter assume that $\varphi(t)$ is an explicit sum of exponentials such that particular time constants in $\varphi(t)$ are associated with distinct relaxation populations. This permits a further discussion as to the use of the logarithmic moments in the analysis of structural heterogeneity and how they can assist in interpretation of temperature and frequency dependences of T_1 relaxation.

2. The *k*-th central logarithmic moment of τ

2.1. Definition

In the following derivation, the nomenclature by Zorn is being used [7]. The k-th logarithmic moment of τ is defined as

$$\langle(\ln\tau)^k\rangle = \int_0^\infty (\ln\tau)^k g(\ln\tau)\, d\ln\tau \tag{1}$$

where τ is generally assumed dimensionless which can be achieved by normalization by a reference time unit. The first moment ($k = 1$) represents the arithmetic mean time on the logarithmic scale. The second central moment ($k = 2$), or the variance of τ on the logarithmic scale,

$$\sigma^2_{\ln\tau} = \langle(\ln\tau)^2\rangle - \langle\ln\tau\rangle^2 \tag{2}$$

is related to the width of $g(\ln\tau)$. And the third central moment ($k = 3$),

$$\mu_{3\ln\tau} = \langle(\ln\tau)^3\rangle - 3\langle(\ln\tau)^2\rangle\langle\ln\tau\rangle + 2\langle\ln\tau\rangle^3, \tag{3}$$

measures skewness, or asymmetry of $g(\ln\tau)$, with a positive value corresponding to a right-skewed (right-tailed) and a negative value to a left-skewed (left-tailed) distribution.

The geometric mean, $\langle\tau\rangle_g$, and the geometric standard deviation, σ_g, of τ are related to respective logarithmic moments as follows:

$$\langle\tau\rangle_g = \exp(\langle\ln\tau\rangle) \tag{4}$$

$$\sigma_g = \exp\left(\sqrt{\sigma^2_{\ln\tau}}\right) \tag{5}$$

The skewness on the logarithmic scale is defined as

$$\gamma_{1\ \ln\tau} = \mu_{3\ln\tau}/\sigma^3_{\ln\tau} \tag{6}$$

Finally, when measuring the relaxation rate r instead of the relaxation time τ, ($r = \tau^{-1}$), one applies $\langle(\ln r)^k\rangle = (-1)^k\langle(\ln\tau)^k\rangle$.

As emphasized in the Introduction, the logarithmic moments of τ can be calculated directly from the relaxation function $\varphi(t)$, that is, without knowing $g(\tau)$. This is made possible by transforming $\varphi(t)$ to a convolution of $g(\tau)$ with one of well-known functions, $f(t)$, such that a moment for g can be calculated from the respective moments for φ and f [7].

2.2. Derivation

Let $\varphi(t)$ be a superposition of exponential relaxation decays with a relaxation time distribution $g(\ln\tau)$ such that $g(\ln\tau)\, d\ln\tau$ is a weight of the components with relaxation times from τ to $\exp(\ln\tau + d\ln\tau)$:

$$\varphi(t) = \int_{-\infty}^{\infty} \exp(-t/\tau)\, g(\ln\tau)\, d\ln\tau \tag{7}$$

Following Ref. [7], we differentiate (7) with respect to $\ln t$,

$$-\frac{d\varphi}{d\ln t} = \int_{-\infty}^{\infty} \exp(\ln t - \ln\tau - \exp(\ln t - \ln\tau))\, g(\ln\tau)\, d\ln\tau, \tag{8}$$

to represent the relaxation data as a convolution of $g(\ln\tau)$ with $f = \exp(x - \exp(x))$. This, in turn, allows us to calculate the moments of g via those of $-d\varphi/d\ln t$ and f using the moment rule for convolution. The rule states that the k-th moment of the convolution $(g * f)(x)$ can be expressed in terms of moments of g and f as [9]:

$$\langle x^k\rangle_{g*f} = \sum_{j=0}^{k} \frac{k!}{j!(k-j)!} \langle x^j\rangle_g \langle x^{k-j}\rangle_f \tag{9}$$

Applying this rule to the convolution (8), one writes for the above-defined moments [7]:

$$\langle\ln\tau\rangle = 0.5772 + \langle\ln t\rangle \tag{10a}$$

$$\sigma^2_{\ln\tau} = \langle(\ln t)^2\rangle - \langle\ln t\rangle^2 - \pi^2/6 \tag{10b}$$

$$\mu_{3\ln\tau} = \langle(\ln t)^3\rangle - 3\langle(\ln t)^2\rangle\langle\ln t\rangle + 2\langle\ln t\rangle^3 + 2.404 \tag{10c}$$

Here, the integral

$$\langle(\ln t)^k\rangle = -\int_{-\infty}^{\infty} (\ln t)^k \frac{d\varphi}{d\ln t}\, d\ln t \tag{11}$$

is the k-th moment calculated with $-d\varphi/d\ln t$ taken as a distribution function while the numerical values 0.5772 and 2.404 are analogous integrals for f [7]. When dealing with experimental data, the integral (11) is defined on the closed interval $[\ln t_1, \ln t_N]$, where t_1 and t_N are the first and the last of N sampling points of φ. Integrating (11) by parts, we obtain in the limit $t_1 \to 0$ and $t_N \to \infty$ a practicable form:

$$\langle(\ln t)^k\rangle = (\ln t_1)^k + k\int_{\ln t_1}^{\ln t_N} (\ln t)^{k-1}\varphi \quad d\ln t \tag{12}$$

Thus, the calculation of the logarithmic moments amounts to a numerical integration of φ given by Eq. (12) and a few elementary operations by Eq. (10). To use these equations implies that φ is sampled at logarithmic steps and normalized to [1, 0].

3. Computational accuracy tests

3.1. The effect of data sampling

Eq. (12) brings in two principle sources of systematic error to the logarithmic moment estimates. One is the sampling interval $[t_1, t_N]$ which defines the integration limits in (12). For a good accuracy, the interval $[t_1, t_N]$ must cover φ up to its asymptotic levels on

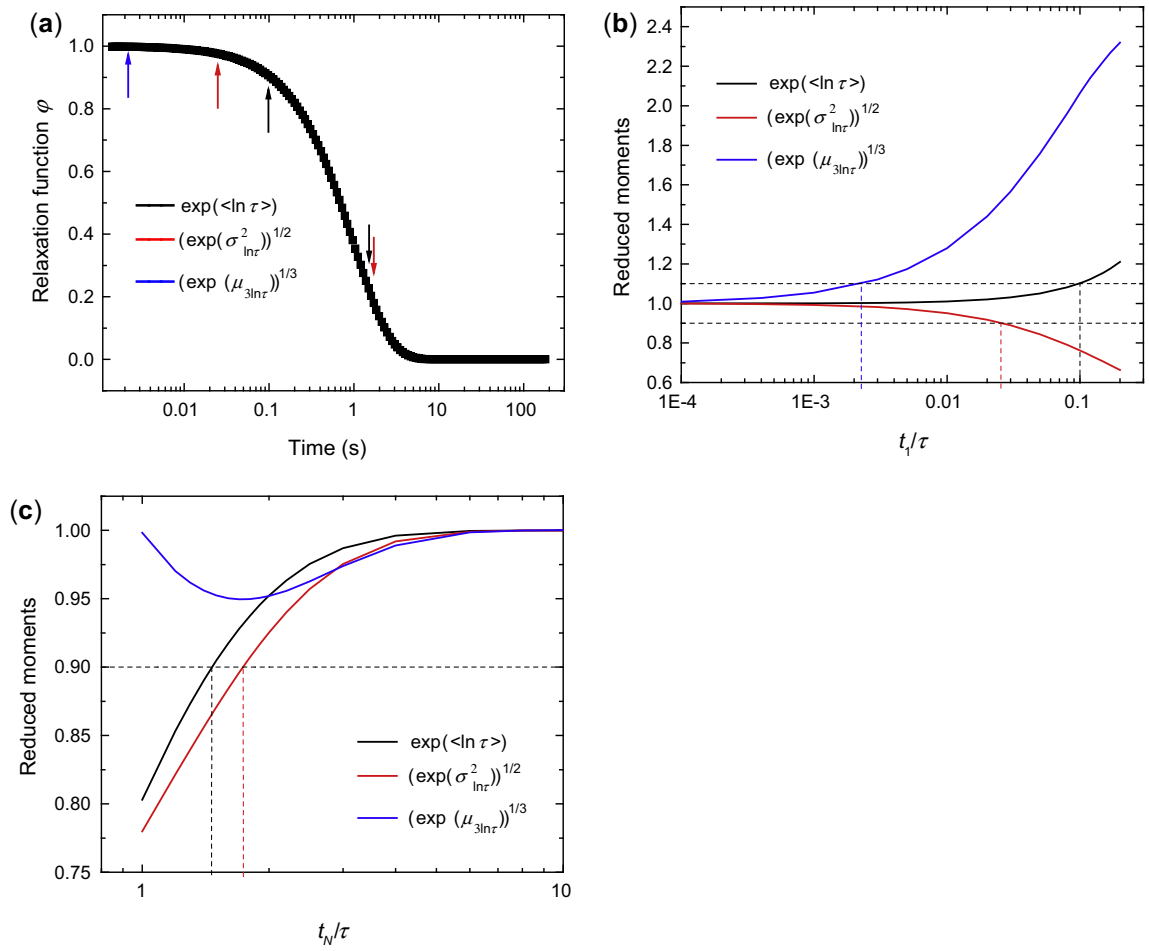

Fig. 1. (a): An example of a mono-exponential relaxation function with $\tau = 1$ s. The arrows shows sampling limits at which respective logarithmic moment estimates deviate from true values by 10% (the truncation error for the 3rd moment is below 10%, hence no arrow shown at long times). (b) and (c): Logarithmic moment estimates reduced toward geometric mean scale as functions of the lower (t_1) and upper (t_N) limits of a sampling interval.

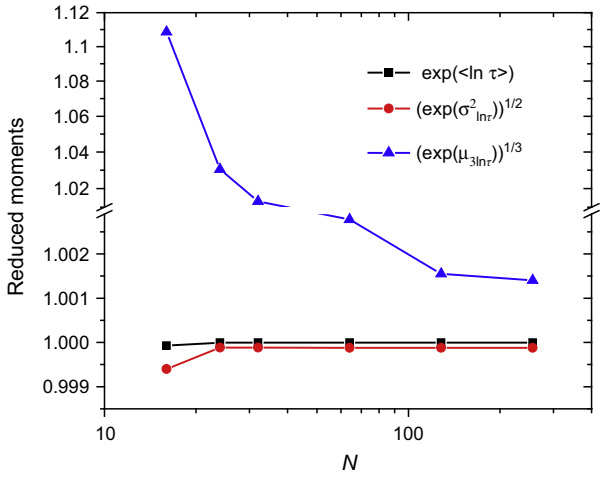

Fig. 2. Logarithmic moment estimates (reduced toward the geometric mean scale) as functions of N, a number of points. None deviates by more than 10% from the true values provided that $N > 20$.

either side of the log-time scale. Fig. 1 illustrates that for a model mono-exponential decay with a time constant $\tau = 1$ s. The error due to the lower limit of t_1 remains below practically acceptable 10% up to $t_1 = 0.1\tau$, 0.025τ, and 0.002τ for the first, the second, and the third moment, respectively. That is, the error due to the late acquisition onset increases with k: it is the least for the first moment, still tolerable when φ drops down to 90% of its amplitude at $t_1 = 0.1\tau$, and it is the most for the third moment which requires, for a good accuracy, that sampling begins at t_1 of three orders of magnitude shorter than τ (Fig. 1a and b). The error due to the upper limit of t_N attains 10% at $t_N = 1.5\tau$ and 1.7τ for the first and the second moments (at which points φ drops down to 22 and 18% of its amplitude, respectively). On the other hand, the third moment does not deviate more than by 5% from the true value (Fig. 1c), thus appearing least affected by an early truncation of φ.

The other accuracy factor is the sampling step $\Delta \ln t$ ($\propto N^{-1}$) which controls the numerical approximation of the integral (12). Fig. 2 shows calculated logarithmic moments of the mono-exponential decay as a function of N for Simpson's rule integration. It appears that N has a significant effect only on $\mu_{3\ln\tau}$, but even in this case the approximation is still passable (10% error) for $N = 16$. We note, however, that one would hardly set N on the basis of the numerical approximation criterion. Rather, one might want N to be as large as possible to minimize the effect of the noise on data normalization and scatter in values (see below), yet keeping the total experiment time reasonably short.

3.2. The effect of noise

The noise present in φ enters (12) with the weight $(\ln t)^{k-1}$, hence its effect depends on k. To appreciate this dependence, let us compute the variance of a weighted sum of N random variables

$$y \equiv \sum_{i=1}^{N} a_i x_i \tag{13}$$

as a representative of the noise term in (12). We assume that x_i are independent random additions to φ_i in (12) and that they are normally distributed with mean 0 and variance σ^2. Then, the variance of the sum (13) is given by [10]

$$\sigma_y^2 \equiv \sigma^2 \sum_{i=1}^{N} a_i^2 \tag{14}$$

For simplicity, let us consider a sampling interval that is symmetric about zero, $\ln t_1 = -\ln t_N$. Then, the weights $a_i = a_i(k)$ can be written simply as:

$$a_i^2(1) = (\Delta \ln t)^2 \tag{15a}$$

$$a_i^2(2) = \frac{1}{4}(\Delta \ln t)^4 i^2 \tag{15b}$$

$$a_i^2(3) = \frac{1}{16}(\Delta \ln t)^6 i^4 \tag{15c}$$

which, after substituting in (11), gives:

$$\sigma_y^2(1) = \sigma^2 (\Delta \ln t)^2 N \tag{16a}$$

$$\sigma_y^2(2) \approx \frac{1}{12}\sigma^2 (\Delta \ln t)^4 N^3 \tag{16b}$$

$$\sigma_y^2(3) \approx \frac{1}{80}\sigma^2 (\Delta \ln t)^6 N^5 \tag{16c}$$

From this example of a zero-symmetric interval, the logarithmic moment estimation error due to the random noise is a power-law function of k, $\sigma_{LM}^2 \propto (\Delta \ln t)^{2k} N^{2k-1}$. Such a strong dependence on k presents us with a problem for measuring $\mu_{3\ln\tau}$ even at a moderate level of noise. There are two options to reduce this error: either through narrowing a sampling interval at the expense of the integration accuracy (see Section 3.1), or by increasing the number of points N, thus prolonging the experiment. For comparison, Eq. (16) gives $\sigma_{LM}^2 \propto [\ln(t_N/t_1)]^{2k}$ for a constant N and $\sigma_{LM}^2 \propto N^{-1}$ in the case of a constant sampling interval.

To illustrate that, we calculate logarithmic moments for a bi-exponential function with equal components' weights and a varied difference in τ (Fig. 3a). The sampling interval was chosen just sufficiently broad in order to exclude significant systematic errors (see Section 3.1). Thus, addition of 1% of a normal noise (SNR = 17) has only a mild effect on $\langle \ln\tau \rangle$ and $\sigma_{\ln\tau}^2$ values, which both remain statistically significant, but has a destructive effect on $\mu_{3\ln\tau}$ (Fig. 3c). The latter can be reduced significantly by narrowing the sampling interval but with an entailing loss of the integral's accuracy manifested as an upward shift of $\mu_{3\ln\tau}$ in Fig. 3d. Fortunately, one can restore the accuracy by extrapolation of data toward zero time (Fig. 3e), as described in the next section. Fig. 3d and f shows the effect of N: using 256 sampling points instead of 24 results in more than a 3-fold decrease in logarithmic moments deviation, in full agreement with Eq. (16).

3.3. The problem of normalization

Scaling $\varphi(t)$ to [1, 0] consists of two steps: a shift of φ by its value at $t \to \infty$ and normalization of thus-shifted φ to its value at $t \to 0$. To obtain these limit values of φ forms a computational problem in its own right. A simple way to do this is to take extreme points of φ (or a mean of two or three of them at either end), but that might not work if φ is too noisy or sampled far off its plateaus. Therefore, it seems more practicable to fit a model exponential function to φ with its amplitude and offset parameters used as variables. We found a tri-exponential function sufficient to approximate φ at either plateau in all our tests, hence we recommend using this function in practice. Including more terms in the fit seems redundant taking into account a fast convergence of the sum of exponentials to φ. One might consider using a bi-exponential fit when relaxation has a pronounced two-component character in order to reduce variability in best-fit parameters. In assessing whether to decrease the number of terms, one can rely on F-test or similar statistical tests to compare nested models.

The advantage of using a model fit function, other than a relatively accurate data normalization, is that it enables extrapolation of φ towards zero time, thus providing a better fulfillment of the limiting conditions underlying Eq. (12). All calculations in this work were, if not mentioned otherwise, performed on extrapolated magnetization curves with N extra values added at the beginning of the curves. Fig. 4 and Table 1 illustrate the benefit of the extrapolation. A ^{7}Li NMR stimulated echo in a lithium-ion conductor shows a prominent two-component decay with a major component (80%) relaxing with τ = 7 μs and a minor component with τ = 0.3 ms (Fig. 4). Because of the extremely fast relaxation of the major component, the signal recorded on delays shorter than 10 μs misses approximately 50% of its total amplitude. Calculation of $\langle \ln\tau \rangle$ and $\sigma_{\ln\tau}^2$ on such incomplete data leads to intolerable errors, especially so for $\sigma_{\ln\tau}^2$. Extrapolation toward zero time gives correct results, as can be ascertained from comparison to a bi-exponential decomposition or more comprehensive ILT analysis (Table 1).

Extrapolation is potentially unsafe in the presence of outlying values, the more as they affect the fit. The logarithmic moments derivation formulated in Section 2.2 allows to omit any value from a given data set, which can be employed to detect the outliers through an abrupt change of the resulting moments. Optionally, one might consider discarding a few data points in the beginning of a relaxation curve to assess how sensitive it is to magnetic field transients upon switching r.f. pulses or the magnet.

4. Further feasibility tests

4.1. Discrimination of two relaxation components

Measuring the logarithmic variance $\sigma_{\ln\tau}^2$ aims to assist in the analysis of structural and dynamical heterogeneity as it manifests itself in relaxation broadening. The sensitivity of $\sigma_{\ln\tau}^2$ to the presence of two relaxation components as a function of their relative intensity and separation was tested on a model spectrum (Fig. 5a) at two levels of noise. The number of data points was chosen to be 32, which is about a typical number used in T_1 relaxometry. The calculations show (Fig. 5b) that for 1% of noise (SNR = 17), $\sigma_{\ln\tau}^2$ differs from zero by a statistically significant amount when relaxation times differ on the logarithmic time scale by a factor of 2 or more. For 5% of the noise (SNR = 3), they are distinguishable when they differ by a factor of 5 to 10, depending on the second component's weight fraction.

For a test on experimental data, a set of T_1-relaxation curves were acquired from a composite sample of cyclohexane and $CuSO_4$-doped water in a wide range of the relaxation field using the field-cycling technique. The fluids were placed in two coaxial NMR tubes and cooled down to T = 273 K so that cyclohexane turned into plastically crystalline phase, while doped water remained unfrozen. This temperature regime provided essentially different T_1 dispersions for the two components with up to a sixty-fold gap between the respective T_1 values (Fig. 6a). (For previous measurements of T_1 dispersion in solid cyclohexane, see [11].) In this test, we measured the geometric standard deviation

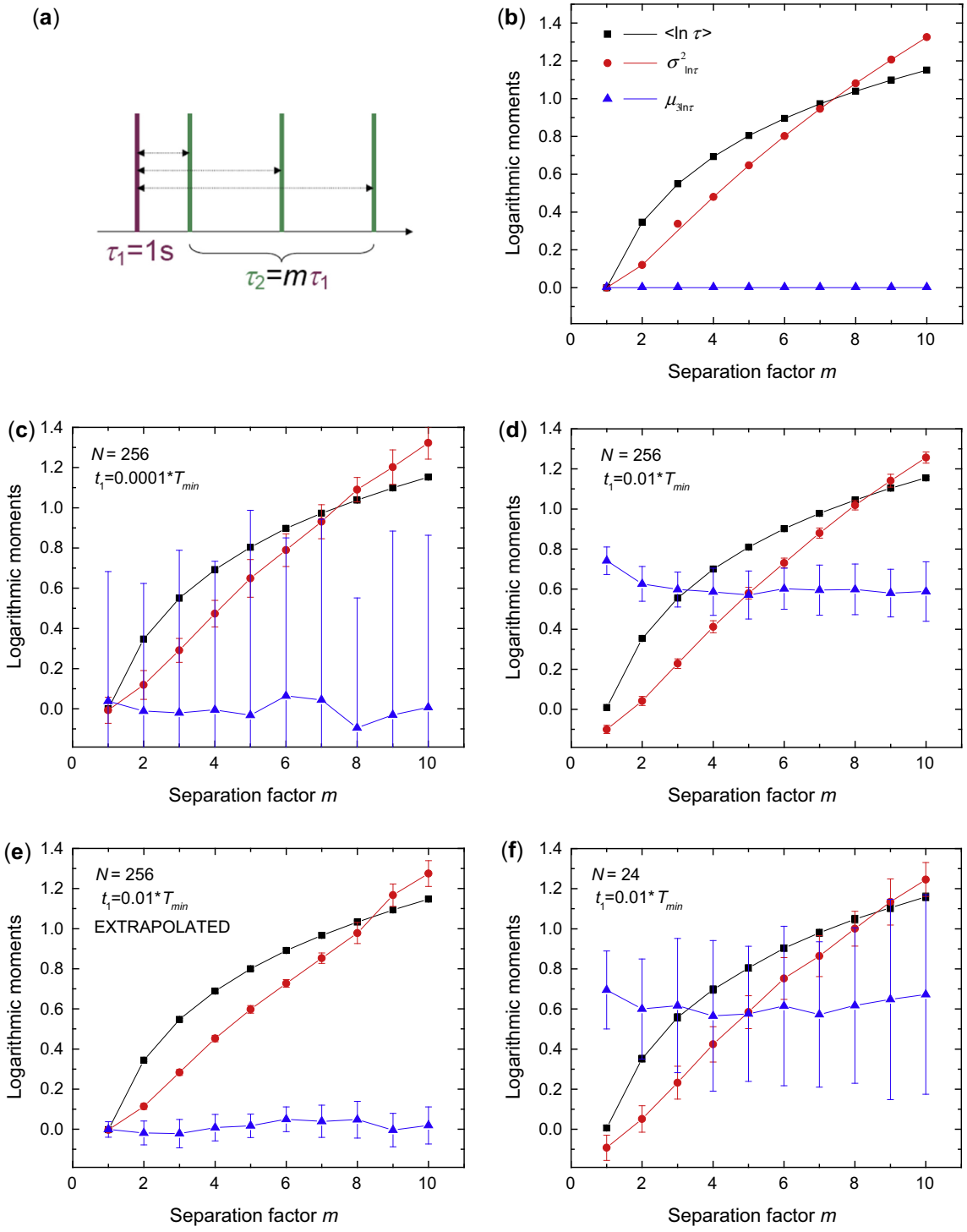

Fig. 3. Effect of noise on the error in logarithmic moment estimates in the case of a two-component relaxation spectrum (a) with a variable component separation m. (b): Mean logarithmic moments values and their standard deviation for noiseless relaxation function, sampled in a wide interval $t_i \in [0.0001T_{min}, 10T_{max}]$, $N = 256$. The solid lines represent theoretical values for the model used. (c) Same sampling conditions as in (b) but with SNR = 17. (d) The sampling interval is set twice as narrow as in (c). (e) The effect of the sampling interval narrowing is compensated by extrapolation beyond the lower limit t_1. (f) The number of points is reduced down to $N = 24$ compared to $N = 256$ in (d). SNR is defined as the ratio of the relaxation function amplitude to the maximum peak-to-peak difference in a normal noise background, which, according to a "3-sigma rule", is taken equal to 6 times the noise's standard deviation.

σ_g which has a theoretical minimum of 1 at the point where two exponential decay time constants coincide. For a reference, we calculated σ_g from known T_1's and an effective component ratio (see Fig. 6a). The substantial change in the component ratio is owing to a partial loss of magnetization during the field switching intervals of several ms. Because of a stronger T_1 dispersion. the weight fraction of cyclohexane decreases more pronouncedly than that of doped water. Fig. 6b shows that except for one outlier, the σ_g measured on the composite sample follows the reference values accurately while remaining sensitive to a difference in T_1 of less than a

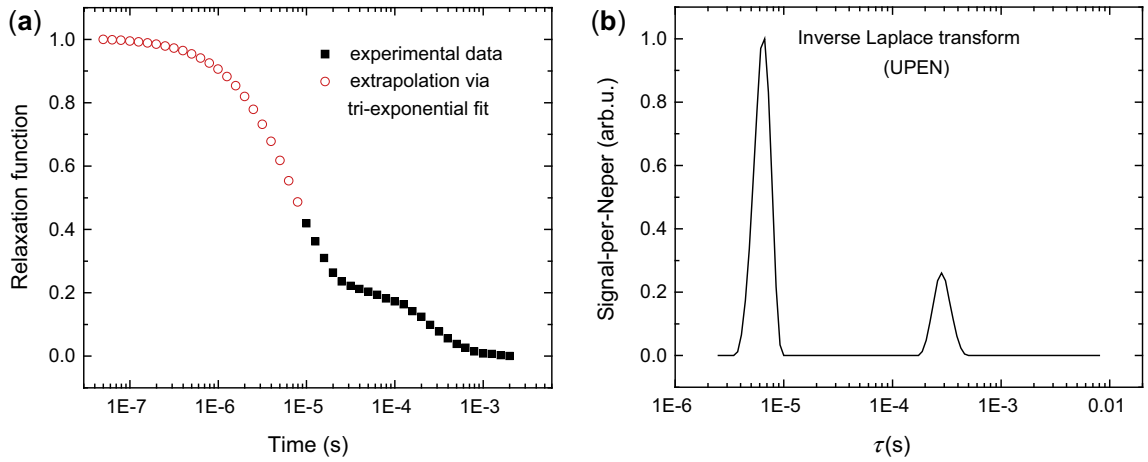

Fig. 4. (a) A ^{7}Li stimulated-echo decay in a lithium-ion conductor (black symbols) and its extrapolated values (red symbols) obtained through a triple-exponential fit. (b): Inverse Laplace transform of the original data (the algorithm UPEN [4]). (For interpretation of the references to colour in this figure legend, the reader is referred to the web version of this article.)

Table 1
The two lowest-order logarithmic moments calculated from $\varphi(t)$ shown in Fig. 4a by this method and through multi-exponential deconvolution of $\varphi(t)$. Missing more than 50% of the signal due to a fast relaxation necessitates data extrapolation.

$\langle \ln\tau \rangle$				$\sigma^2_{\ln\tau}$			
This method		UPEN	Bi-exponential	This method		UPEN	Bi-exponential
Without extrapolation	After extrapolation			Without extrapolation	After extrapolation		
−10.172	−11.111	−11.183	−11.119	0.082	2.368	2.447	2.406

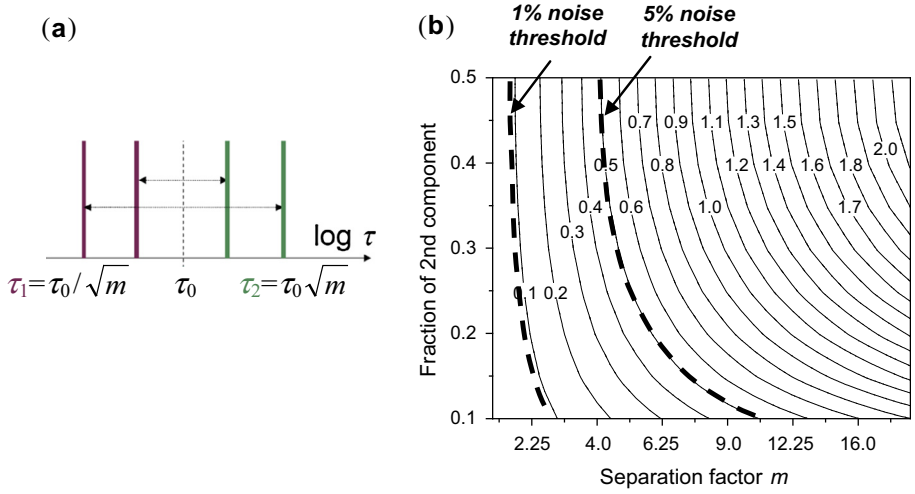

Fig. 5. (a) A two-peak relaxation spectrum with a centre of gravity fixed. (b) The logarithmic variance of (a) calculated for various peak separations and height ratios (N = 32).

factor of two (Fig. 6b). Measurements on data acquired with a finer relaxation field increment and in the immediate vicinity of a σ_g minimum (not plotted here) show that the deviation of σ_g from 1 becomes statistically significant when T_1 values differ by 30%. We note that this figure is less than the thresholds reported above for model spectra (see Fig. 5), apparently due to a better SNR in the experimental data used.

4.2. Comparison with the ILT analysis

Fig. 7a shows $g(\ln T_1)$ obtained through the Inverse Laplace Transform of the data used in the previous test. The geometric mean $\langle T_1 \rangle_g$ and the geometric standard deviation σ_g calculated from thus obtained $g(\ln T_1)$ are drawn in Figs. 6b and 7b along with respective values from the logarithmic moment analysis. The results by the two methods are virtually identical. It is worth mentioning that the employed ILT algorithm (UPEN [4]) provides correct integral characteristics of $g(\ln T_1)$ even though it does not resolve it into separate peaks unless their T_1 values differ by more than a factor of six (see Fig. 7a).

Fig. 7c relates the skewness parameter $\gamma_{1\ \ln T_1}$ calculated from the logarithmic moments analysis to the shape of $g(\ln T_1)$ given by ILT. As expected, $\gamma_{1\ \ln T_1}$ turns from positive to negative values as $g(\ln T_1)$ changes from a right-tailed to a left-tailed distribution.

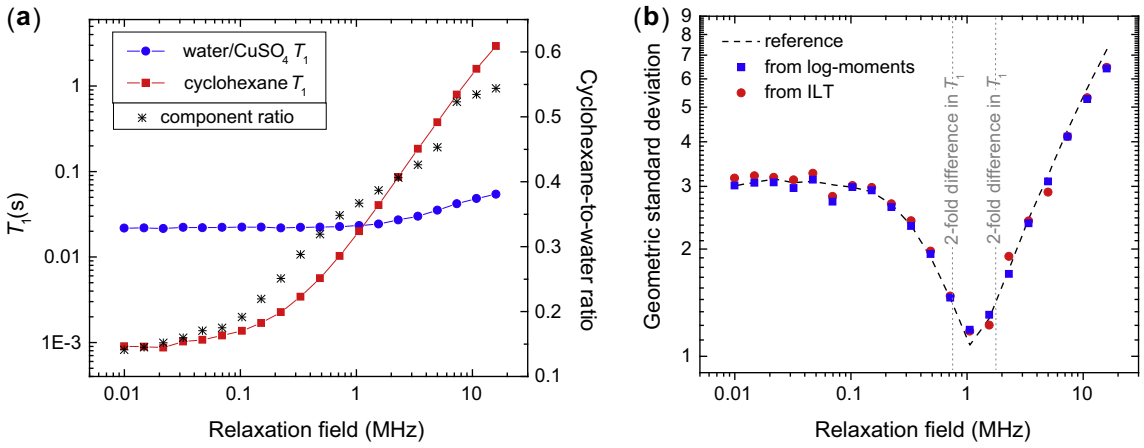

Fig. 6. (a) T_1 values and an effective FID amplitude ratio of $CuSO_4$-doped water and frozen cyclohexane which served as composite sample's components in the discrimination test. Due to an uneven signal attenuation upon varying the relaxation field strength, the cyclohexane-to-water ratio changes from 0.54 at 16 MHz down to 0.14 at 10 kHz (see text). (b) Geometric standard deviation σ_g as the measure of component separation calculated from composite sample's data. The values calculated from ILT are shown for comparison (see also Fig. 7).

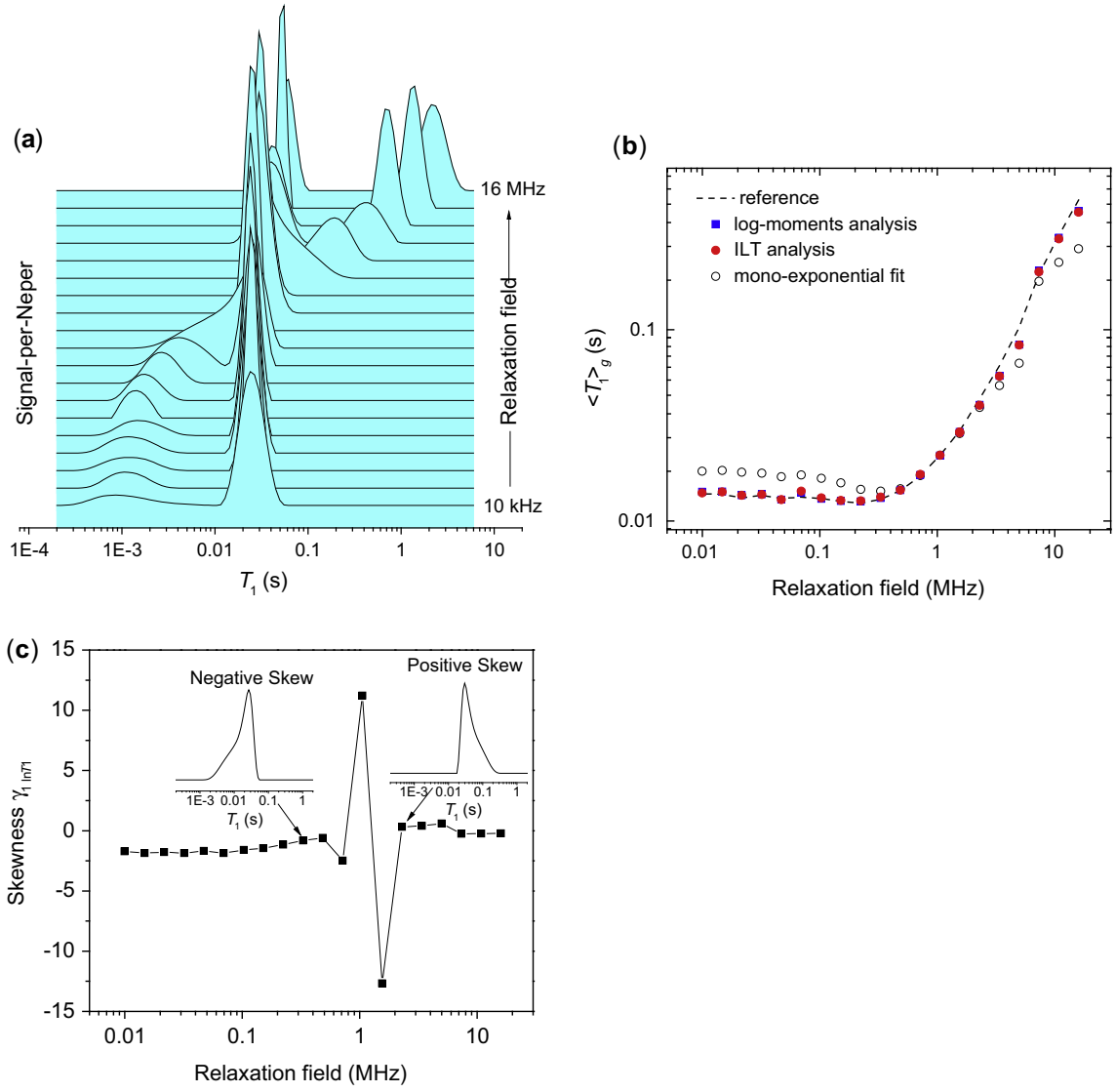

Fig. 7. (a) T_1 distributions by ILT (the UPEN algorithm) in the composite sample of $CuSO_4$-doped water and cyclohexane (see text) (b) The geometric mean T_1 calculated from ILT shown in (a) compared to the corresponding quantity from the logarithmic moment calculation and the best-fit time decay constant of a mono-exponential model. (c) The skewness parameter $\gamma_{1\ln T1}$ from the logarithmic moment calculation.

At the crossover, where $g(\ln T_1)$ collapses down to a single peak, both numerator and denominator in Eq. (6) approach zero. This is likely to explain the vast $\gamma_{1\ \ln T_1}$ fluctuations around 1 MHz.

4.3. Comparison with the stretched exponential analysis

The stretched exponential function (17), also called the Kohlrausch function, is a long-used, compact model for phenomenological description of non-exponential relaxation, also in NMR relaxometry [12–14].

$$\varphi(t) \propto \exp[-(t/\tau_K)^{\beta}] \tag{17}$$

A stretching exponent $\beta \in [0, 1]$ measures the deviation from a mono-exponential relaxation, with $\beta = 1$ corresponding to the usual exponential function. As such, β has to correlate inversely with σ_g. The first moment of a normalized (17)

$$\langle\tau\rangle = \int_0^{\infty} \exp[-(t/\tau_K)^{\beta}]\,dt = \frac{\tau_K}{\beta}\Gamma\left(\frac{1}{\beta}\right) \tag{18}$$

where Γ is the gamma function, is interpreted as a mean relaxation time and is to be compared to $\langle\tau\rangle_g$. To draw the comparison, we utilize ^{1}H T_1 relaxation data acquired by the field-cycling technique from commercially available dry-cured ham (Jamón Serrano, Spain). Samples were cut from the representative muscle and adipose regions of ham slices and measured at 10 °C in the relaxation field ranging from 20 MHz down to 10 kHz. The muscle tissue shows a nearly mono-exponential T_1 relaxation, with the σ_g values not exceeding 1.6 (Fig. 8a). Accordingly, fitting (17) to the data yields the stretching exponent β that is close to 1 (Fig. 8b). A slight deviation from an exponential is positively seen in both σ_g and β graph near the relaxation field of 1 MHz. Whatever causes this deviation is fairly measurable through the geometric standard deviation and the stretching exponent values, even though a mono-exponential fit appears as good as everywhere else. The adipose tissue exhibits essentially a non-exponential relaxation. The σ_g values monotonically grows from 1.6 at 20 MHz up to 2.1 at 10 kHz (Fig. 8c). The β values follows same trends as in σ_g, recalling their inverse correlation (Fig. 8d). Thus, given comparable scatter in values, either of these quantities can be used to detect relaxation broadening. We note, however, that relation of β to the second moment of T_1 is regarded as being mostly qualitative because of the phenomenological concept of the stretched exponential model. Besides, the goodness of fit of (17) might be an issue, *e.g.*, for data with a bimodal $g(\tau)$.

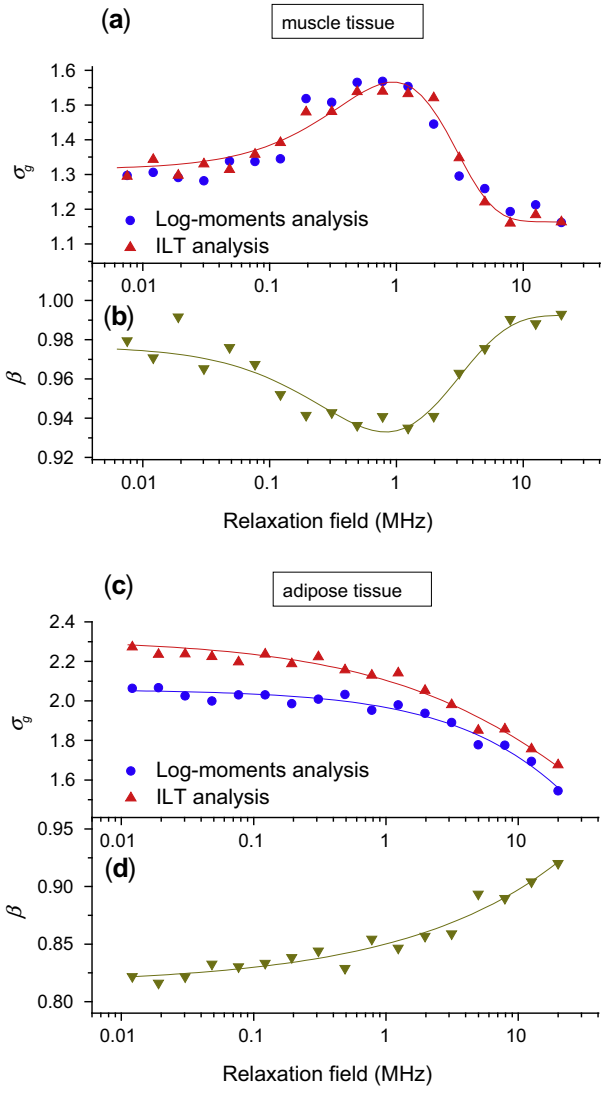

Fig. 8. (a) The geometric standard deviation σ_g by the logarithmic moment analysis (circles) and by ILT (triangles) of the data collected from muscle tissue of a dry-cured ham sample, as a function of the relaxation field strength. (b) Corresponding best-fit stretching exponent β in Eq. (17). (c and d) Same quantities but measured on adipose tissue. The solid lines are a guide to the eye.

The stretched-exponential model gives the mean T_1 that coincides with the corresponding value from the logarithmic moment analysis in the case of the muscle tissue, but is significantly greater for the adipose tissue (Fig. 9). This can be explained taking into account that the integral (18) defines the mean on a linear timescale, that is, the usual arithmetic mean $\langle T_1\rangle_a$, for which the general inequality $\langle T_1\rangle_a \geqslant \langle T_1\rangle_g$ applies, the more so as relaxation deviates from an exponential. A dip is visible on the T_1 dispersion curve of the muscle tissue at 2 MHz, owing to a quadrupolar enhancement of the ^{1}H relaxation in a vicinity of immobilized proteins' amino-groups [15].

Although it is not immediately relevant to the present discussion, we note that combining the logarithmic moment and stretched exponential analysis allows one to calculate the harmonic mean $\langle T_1\rangle_h$ using the relationship $\langle T_1\rangle_a \langle T_1\rangle_h = \langle T_1\rangle_g^2$ [16]. The harmonic mean is of particular use in studying glass transitions, as this quantity exhibits no (misleading) discontinuity at the relaxation crossover from slow to fast exchange limit [13]. Usually, $\langle T_1\rangle_h$ is measured from a time derivative of $\varphi(t)$ at $t \to 0$, which requires high-precision magnetization curves. Here $\langle T_1\rangle_h$ is calculated from integral values which are far less demanding of SNR.

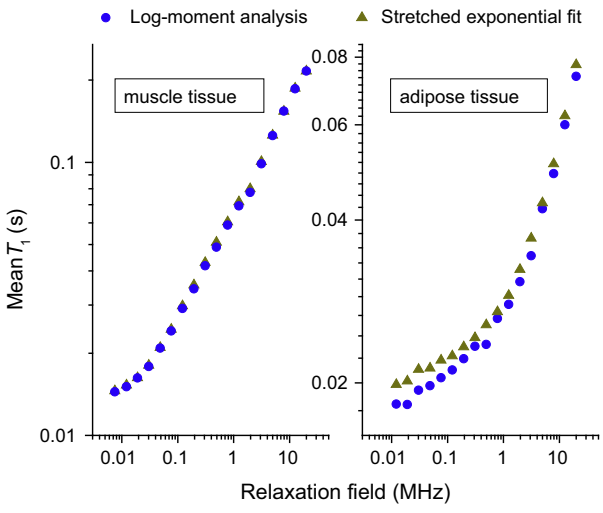

Fig. 9. Mean T_1 in dry-cured ham samples obtained via the logarithmic moments analysis (circles) and the stretched exponential fit (triangles).

Fig. 8c shows the trend which is commonly seen when comparing σ_g values by ILT and by the logarithmic moment analysis. Namely, ILT gives σ_g that is greater than a corresponding quantity obtained from the logarithmic moments calculation. We attribute this to regularization in ILT which leads to artificially broadened distributions and thus results in overestimated σ_g values.

5. Discussion and conclusion

Let us emphasize benefits of the logarithmic moments when keeping track of non-exponential behavior of $\varphi(t)$. Besides the computational advantages, there are a number of arguments, some being supported by the present data and others being only a claim, in favor of using the moments defined on the logarithmic scale.

(i) The relaxation function $\varphi(t)$ is often sampled at logarithmically equidistant points, whenever it is possible, to capture better its exponential behavior, with a rapid change at short times and a progressively slower change on longer times. Having been plotted against ln t, the thus sampled $\varphi(t)$ appears as a smooth-step function with a well visible inflection point and a slope enabling easy comparison of data in terms of the mean relaxation time and its deviation form exponential (see, *e.g.*, Figs. 1a and 4a). On the other hand, ILT algorithms output relaxation time distributions as histograms on a logarithmic abscissa. That makes sense since it is the ratio of relaxation times rather than their difference that defines the non-exponential character of relaxation. It is fitting therefore that one deals with quantities measured on the logarithmic time scale whenever comparing to those, popular, representations of relaxation data.

(ii) The geometric mean $\langle\tau\rangle_g$ is preferable to the usual arithmetic mean $\langle\tau\rangle_a$ as a characteristic relaxation time of highly skewed τ distributions. When τ values differ by a factor of 10 or more, $\langle\tau\rangle_a$ is dominated by a longer-τ component even if it is comparable to shorter-τ constituents by weight. In some extreme situations, such as encountered in relaxation of fluids in porous media with a bulk fraction present, $\langle\tau\rangle_a$ may address neither of the relaxation components and therefore cannot represent a characteristic relaxation time in the sense of the most frequent value. The geometric mean seems to be a more balanced quantity for such cases.

(iii) The logarithmic moments are particularly convenient for analysis of variable-temperature T_1 measurements. In a simple case of thermal fluctuations characterized by a single correlation time τ_c, T_1 is proportional to $\tau_c\omega^2$ and τ_c^{-1} in the slow and fast motion limits, respectively, such that the dependence of T_1 on temperature takes the Arrhenius form for a given activation barrier E. Let us now assume that there is a distribution of activation barriers, $G(E)$, leading to a respective distribution of T_1. Then the variance of E is related to the log-variance of T_1 simply as $\sigma_E = k_B\sigma_{\ln T1}T$ [7], such that the product $\sigma_{\ln T1}T$ is invariant to T unless $G(E)$ changes with temperature. By monitoring the $\sigma_{\ln T1}T$ value, one can readily explore whether such a change takes place, *e.g.*, as a result of structural rearrangement or a chemical reaction.

(iv) Measuring $\sigma_{\ln T1}$ may also assist in the analysis of T_1 as a function of the relaxation field strength (T_1 dispersion). Provided that the relaxation function is a sum of terms with Lorentzian-like dispersions, $\sigma_{\ln T1}$ is to be invariant to the field strength in the high and low field limits. The observation of $\sigma_{\ln T1}$ that does vary in those extreme fields would either indicate an exchange between relaxation components or call for a model that exploits a non-Lorentzian dispersion.

Despite the simplicity of the general approach, the calculation of the logarithmic moments has two methodological shortcomings. One lies in the need, as a preliminary, of data normalization, which relies on the choice of the objective function as well as on the employed optimization technique (see Section 3.3). A poor data quality and incomplete sampling of φ at its long-time plateau can readily make normalization a principle source of error, especially so for field-cycling relaxation data with their intrinsically non-zero offsets. The other problem is the requirement for φ to be sampled in logarithmically equispaced steps. This presents no trouble in convenient T_1 relaxometry and diffusometry, but may be difficult to achieve in the experiments based on Carr-Purcell-Meiboom-Gill (CPMG) and similar pulse sequences with a constant acquisition period. Further work to overcome this problem will be necessary. (In view that CPMG T_2-decays comprise many points and only a few are required for the log-moment calculation, it seems possible to interpolate φ for the logarithmically equispaced time delays.)

The estimation of $\langle\ln\tau\rangle$ and $\sigma^2_{\ln\tau}$ has proved robust against deficiencies of the experiment such as a small number of data points and scatter in values. The quantities will assist in analyzing structural and dynamical heterogeneities and in studying magnetization exchange processes. The calculation of $\mu_{3\ln\tau}$ was found to be less reliable due to its particular susceptibility to the noise and therefore must be used with caution. In many aspects, measuring logarithmic moments on $\varphi(t)$ is a computationally facile alternative to the Inverse Laplace Transform of data. It is worth noting, however, that it gives information only about integral characteristics of an underlying distribution of exponentials such that no information on the distribution's modality is provided. If one's objective is to know whether the distribution breaks up into two or more peaks, suggesting separate populations, then one should consider using ILT (with a carefully adjusted regularization parameter) or else exploit the tools that are especially designed for separating exponential components [17].

6. Experimental

The field-cycling measurements of ^{1}H T_1 relaxation decays were carried out on a Stelar Spinmaster FFC2000 relaxometer, at T = 273 K. The detection field was 17 MHz, while the relaxation field varied from 16 to 0.01 MHz, the field switching time 2.5 ms, the pre-polarization at 20 MHz took 1.9 s, and the 90°-pulse was 7.5 μs long. A composite test sample for these measurements was made of two nested coaxial NMR tubes of 5 and 10 mm diameters, filled with cyclohexane and $CuSO_4$-doped water, respectively, in the proportion that gave equal signal intensities at the maximum relaxation field used in this experiment (16 MHz). Dry-cured ham (Jamón Serrano, Spain) was purchased from a local vendor in a form of thin slices. The muscle and adipose tissue were separated by a knife and packed in 10 mm NMR tubes without further treatment.

The Inverse Laplace Transform algorithm used was UPEN [4] featuring a uniform penalty smoothing of distribution components. A regularization parameter was kept close to its limit (about 3 times the default value) to minimize a line broadening yet preventing instability in data inversion.

The logarithmic moment computation algorithm was written in the programming language Python. The program includes the triple-exponential fit by the Powell's optimization method for data scaling and extrapolation purposes, which was implemented using the lmfit package.

Acknowledgments

This project has received funding from the European Union's Horizon 2020 research and innovation programme under grant

agreement No 668119 (project "IDentiFY"). We thank Dr. Reiner Zorn for helpful comments on his article [7]; Dr. Oliver Neudert and Dr. Carlos Mattea for introduction to the field-cycling relaxometry and their suggestions about a test sample; and Prof. Dr. Michael Vogel for permission to use the ^{7}Li stimulated-echo data.

References

[1] J.J. Howard, W.E. Kenyon, Determination of pore size distribution in sedimentary rocks by proton nuclear magnetic resonance, Mar. Pet. Geol. 9 (1992) 139–145.
[2] G.R. Coates, L. Xiao, M.G. Prammer, N.M.R. Logging, Principles & Applications, Halliburton Energy Services, Houston, 1999.
[3] D.E. Freed, Dependence on chain length of NMR relaxation times in mixtures of alkanes, J. Chem. Phys. 126 (2007) 174502.
[4] G.C. Borgia, R.J.S. Brown, P. Fantazzini, Uniform-penalty inversion of multiexponential decay data, J. Magn. Reson. 132 (1998) 65–77.
[5] L. Venkataramanan, Y.-Q. Song, M.D. Hürlimann, Solving fredholm integrals of the first kind with tensor product structure in 2 and 2.5 dimensions, IEEE Trans. Signal Process. 50 (2002) 1017–1026.
[6] B. Kaulakys, V. Gontis, M. Alaburda, Point process model of 1/f noise vs a sum of Lorentzians, Phys. Rev. E 71 (2005) 051105.
[7] R. Zorn, Logarithmic moments of relaxation time distributions, J. Chem. Phys. 116 (2002) 3204–3209.
[8] G.C. Borgia, V. Bortolotti, R.J.S. Brown, P. Fantazzini, A robust method for calculating geometric mean times from multiexponential relaxation data, using only a few data points only a few elementary operations, Magn. Reson. Imaging 14 (1996) 895–897.
[9] C.A. Laury-Micoulaut, The n-th centered moment of a multiple convolution and its applications to an intercloud gas model, Astron. Astrophys. 51 (1976) 343–346.
[10] E.W. Weisstein, Normal sum distribution, From *MathWorld* – A Wolfram Web Resource. <http://mathworld.wolfram.com/NormalSumDistribution.html>.
[11] S. Stapf, R. Kmmich, Translational versus rotational molecular dynamics in plastic crystals studied by NMR relaxometry and diffusometry, Mol. Phys. 92 (1997) 1051–1060.
[12] W. Schnauss, F. Fujara, H. Sillescu, The molecular dynamics around the glass transition and in the glassy state of molecular organic systems: a 2H-nuclear magnetic resonance study, J. Chem. Phys. 97 (1992) 1378–1389.
[13] B. Geil, G. Hinze, Influence of data treatment on the shape of 2H NMR T1 curves, Chem. Phys. Lett. 216 (1993) 51–55.
[14] M. Peyron, G.K. Pierens, A.J. Lucas, L.D. Hall, R.C. Stewart, The modified stretched-exponential model fro characterization of NMR relaxation in porous media, J. Magn. Reson., Ser. A 118 (1996) 214–220.
[15] F. Bajd, A. Gradisek, T. Apih, I. Sersa, Dry-cured ham tissue characterisation by fast field cycling NMR relaxometry and quantitative magnetization transfer, Magn. Reson. Chem. 54 (2016) 827–834.
[16] P.S. Bullen, D.S. Mitrinovic, M. Vasic, Means and Their Inequalities, Springer Science & Buisness Media, 2013.
[17] W. Windig, B. Antalek, Direct exponential curve resolution algorithm (DECRA): a novel application of the generalized rank annihilation method for a single spectral mixture data set with exponentially decaying contribution profiles, Chemometr. Intell. Lab. Syst. 37 (1997) 241–254.